

Unprecedented hetero-geometric discrete copper(II) complexes: Crystal structure and bio-mimicking of Catecholase activity

ABHRANIL DE^a, DHANANJAY DEY^a, HARE RAM YADAV^b, MILAN MAJI^c,
VINAYAK RANE^d, R M KADAM^d, ANGSHUMAN ROY CHOUDHURY^b and
BHASKAR BISWAS^{a,*}

^aDepartment of Chemistry, Raghunathpur College, Purulia, West Bengal, 723 133 India

^bDepartment of Chemical Sciences, Indian Institute of Science Education and Research Mohali, Sector 81,
S A S Nagar, Manauli P. O. Mohali, Punjab, 140 306, India

^cDepartment of Chemistry, National Institute of Technology, Mahatma Gandhi Avenue, Durgapur,
West Bengal, 713 209, India

^dRadiochemistry Division, Bhabha Atomic Research Centre, Trombay, Mumbai, Maharashtra 400 085, India
e-mail: icbbiswas@gmail.com; mr.bbiswas@rediffmail.com

MS received 30 March 2016; revised 22 June 2016; accepted 5 September 2016

Abstract. An unprecedented solid of copper(II) complexes, $[\text{Cu}(\text{dpa})_2\text{NCS}]_2[\text{Cu}(\text{dpa})_2(\text{NCS})_2](\text{ClO}_4)_2$ (**1**) [dpa = 2,2'-dipyridylamine; SCN = thiocyanate], has been synthesized and crystallographically characterized with the aim to study the catecholase activity. The Cu(II) complex mimics the full catalytic cycle of the active site of catechol oxidase enzyme in acetonitrile medium with a turnover number of $4.788 \times 10^3 \text{ h}^{-1}$ along with the production of semiquinone radical and hydrogen peroxide. *In situ* generation of Cu(I) species in the catalytic pathway of catechol oxidation was established by electrochemical study and further confirmed by electron paramagnetic resonance (EPR) spectroscopy.

Keywords. Copper; X-ray structure; radical activity; catechol oxidase activity.

1. Introduction

The efficiency and selectivity of copper proteins to process dioxygen has received considerable attraction to synthetic coordination chemists for the investigation of spectroscopic, structural and catalytic properties.¹ Bio-catalysis mediated by copper complexes at ambient conditions is at the fundamental stage in Bioinorganic chemistry. Transition metal ions in oxidase or oxygenase serve to activate the kinetically inert O_2 , and is used to mediate multi-electron redox reactions.^{2,3} Thus, it is of paramount interest to understand the basic functional principles that govern such bi- or poly-metallic reactivity of natural enzymes. Dicopper sites play a pivotal role in biological oxidation and, consequently, the understanding of structural and functional aspects of copper metalloenzymes is a subject of intensive research.^{4–7} A prominent member of these copper proteins is catechol oxidase, which is a type 3 copper protein⁸ and catalyzes exclusively the oxidation of catechols to the corresponding *o*-quinones.

On the other hand, the catecholase activity by various dicopper compounds with different structural

connectivities has been widely investigated.⁹ Mononuclear copper(II) complexes,¹⁰ a few copper(II) clusters and polymers have been found to be active catalysts.^{11,12} Explorations of catecholase activity by new types of compounds are very much demanding. Murphy *et al.*,¹³ Arriortua *et al.*,¹⁴ and Sletten *et al.*,¹⁵ have reported the same class of copper(II) complexes containing dipyridylamine and thiocyanate ions but none of these groups till date have been able to explore the catecholase activity using such Cu(II) complexes as active catalytic system. Herein, we report the addition of a new catalytic system in the form of discrete hetero-geometric copper(II) complex, $[\text{Cu}(\text{dpa})_2\text{NCS}]_2[\text{Cu}(\text{dpa})_2(\text{NCS})_2](\text{ClO}_4)_2$ (**1**) [dpa = 2,2'-dipyridylamine; NCS = thiocyanate], which also potentially mimics the full catalytic cycle of functional models of the active site of catechol oxidase enzyme with significant turnover number along with the production of semiquinone and hydrogen peroxide. The generation of Cu(I) species in the catalytic pathway established by electrochemical analysis was further confirmed by electron paramagnetic resonance (EPR) spectroscopy. EPR titration suggests that the generation of radical of catechol in presence of copper complex is playing a key role towards the catecholase-like activity.

*For correspondence

2. Experimental

2.1 Materials

High purity 2,2'-dipyridylamine (Aldrich, UK), copper(II) perchlorate hexahydrate (Fluka, Germany), ammonium thiocyanate chloride (E. Merck, India), 3,5-di-*tert*-butylcatechol (Sigma Aldrich Corporation, St. Louis, MO, USA), and all other materials were obtained from commercial sources and used as received. All other chemicals and solvents were of analytical grade and were used as received without further purification.

Caution! Perchlorate salts of metal ions are potentially explosive, especially in the presence of organic ligands. Only a small amount of material should be prepared and it should be handled with care.

2.2 General synthesis of the copper(II) complex (**1**)

The discrete hetero-geometric copper complex was synthesized by dropwise addition of aqueous solution of dipyridylamine (0.342 g, 2 mmol) into a solution of $\text{Cu}(\text{ClO}_4)_2 \cdot 6\text{H}_2\text{O}$ (0.365 g, 1 mmol) in the same solvent (20 mL) keeping the solution on magnetic stirrer with slow stirring (450 rpm). Then solid ammonium thiocyanate (0.076 g, 1 mmol) was added as solid into the blue solution and stirring continued to 30 minutes more. The blue solution turned into green and the supernatant liquid was kept in air for slow evaporation. After 7–10 days, fine microcrystalline compound **1** was separated out, which was washed in hexane and dried *in vacuo* over silica gel indicator. The spectroscopic measurements and elemental analyses confirmed the structural formation of the complex. Yield = 0.2870 g, (65.1% based on metal salt and thiocyanate). Anal. calc. (%) $\text{C}_{64}\text{H}_{54}\text{N}_{22}\text{Cl}_2\text{O}_8\text{S}_4\text{Cu}_3$ (**1**): C, 46.61; H, 3.30; N, 18.69; Found (%): C, 46.66; H, 3.24; N, 18.73. Selected IR bands (KBr pellet, cm^{-1}): 3353 (s), 2142 (s), 1426 (m), 1616 (s), 1096 (s). UV-Vis (λ , nm; 10^{-4} M, 1 cm cell, abs): 250–269 (4.068), 290–320 (3.7201), ~397 (0.1688), ~682 (0.0216) (broad); ESI-MS (MeCN): m/z , 235.95 (calcd. 235.75) $[\text{Cu}(\text{dpa})]\text{H}^+$; m/z , 525.91 (calcd. 525.05) $[\text{Cu}(\text{dpa})_2(\text{NCS})_2]\text{H}^+$.

2.3 Physical measurements

Infrared spectrum (KBr) was recorded with a FTIR-8400S SHIMADZU spectrophotometer in the range 400–3600 cm^{-1} . ^1H NMR spectrum in $\text{DMSO}-d_6$ was obtained on a Bruker Avance 300 MHz spectrometer at 25°C and was recorded at 299.948 MHz. Absorption spectra were recorded with a Jasco model V-730

UV-Vis spectrophotometer. Elemental analyses were performed on a Perkin Elmer 2400 CHN microanalyser. Electrospray ionization (ESI) mass spectrum was recorded on a Q-TOF Micro™ Mass Spectrometer. Cyclic voltammograms were recorded in CH_3CN solutions containing 0.1 M TBAP at 25°C using a three-electrode configuration (Pt working electrode, Pt counter electrode, Ag/AgCl reference) and a PC-controlled PAR model 273A electrochemistry system. All the experimental solutions were degassed for 30 minutes with high-purity argon gas. The Electron Paramagnetic Resonance (EPR) spectrum was recorded on a Bruker EMX-X band spectrometer (Model: EMX).

2.4 X-ray diffraction

Single crystal X-ray diffraction data of the copper complex were collected using a Rigaku XtaL ABmini diffractometer equipped with Mercury CCD detector. The data were collected with graphite monochromated Mo-K α radiation ($\lambda = 0.71073 \text{ \AA}$) at 293(2) K using ω scans. The data were reduced using Crystal Clear suite 2.0.¹⁶ and the space group determination was done using Olex². The structure was resolved by direct method and refined by full-matrix least-squares procedures using the SHELXL-2014/7¹⁷ software package using OLEX2 suite.¹⁸ The crystallographic bond distance and bond angle were calculated using PARST¹⁹ and given in Tables 1 and 2, respectively.

Table 1. Crystallographic parameters for **1**.

Crystal parameters	1
Empirical formula	$\text{C}_{64}\text{H}_{54}\text{N}_{22}\text{Cl}_2\text{O}_8\text{S}_4\text{Cu}_3$ 1649.08
Formula weight	293(2) K
Temperature	0.71073 \AA
Wavelength	Monoclinic
Crystal system	$P2_1/c$
Space group	$a = 12.7156(8) \text{ \AA}$ $\alpha = 90^\circ$
Unit cell dimensions	$b = 14.4230(9) \text{ \AA}$ $\beta = 93.802^\circ(3)$ $c = 19.3355(12) \text{ \AA}$ $\gamma = 90^\circ$
Volume	$3538.3(4) \text{ \AA}^3$
Z	8
Density (calculated)	1.548 g cm^{-3}
Absorption coefficient	1.158 mm^{-1}
F(000)	1682
Theta range for data collection	3.0 to 27.5°
Reflections collected	35795
Independent reflections	7978
R(int)	0.056
R indices (all data)	$R1 = 0.0761$, $wR2 = 0.2239$
Largest diff. peak and hole	1.31 and $-0.92 \text{ e. \AA}^{-3}$

Table 2. Bond angle and bond distances of **1**.

Bond distances			
Cu2-N8	2.020(3)	Cu1-N7	1.995(4)
Cu2-N10	2.004(3)	Cu1-N3	2.138(4)
Cu2-N11_b	2.494(6)	Cu1-N4	1.992(4)
Cu2-N11_c	2.494(6)	Cu1-N1	2.020(4)
Cu2-N8_d	2.020(3)	Cu1-N6	2.012(4)
Cu2-N10_d	2.004(3)		
Bond angles			
N8-Cu2-N10	85.46(14)	N10_d-Cu2-N11_b	85.56(17)
N8-Cu2-N11_b	89.40(17)	N8_d-Cu2-N11_c	89.40(17)
N8-Cu2-N11_c	90.60(17)	N10_d-Cu2-N11_c	94.45(17)
N8-Cu2-N8_d	180.00	N8_d-Cu2-N10_d	85.46(14)
N8-Cu2-N10_d	94.54(14)	N3-Cu1-N6	100.73(16)
N10-Cu2-N11_b	94.45(17)	N3-Cu1-N7	102.76(17)
N10-Cu2-N11_c	85.56(17)	N4-Cu1-N6	88.26(16)
N8_d-Cu2-N10	94.54(14)	N4-Cu1-N7	87.73(17)
N10-Cu2-N10_d	180.00	N6-Cu1-N7	156.45(18)
N11_b-Cu2-N11_c	180.00	N1-Cu1-N6	93.11(14)
N8_d-Cu2-N11_b	90.60(17)	N1-Cu1-N7	86.26(15)
N3-Cu1-N4	103.79(16)	N1-Cu1-N3	87.71(15)
N1-Cu1-N4	167.97(15)		

2.5 Catalytic oxidation of 3,5-DTBC

In order to study the catecholase activity of the complex, a 10^{-4} M solution of **1** in acetonitrile was treated with 100 equiv. of 3,5-di-*tert*-butylcatechol (3,5-DTBC) under aerobic conditions at room temperature. Absorbance vs. wavelength (wavelength scans) of these solutions were recorded at a regular time interval of 5 min in the wavelength range 300–900 nm.

The kinetics of oxidation of 3,5-DTBC were determined by the method of initial rates and monitored the growth of the quinone band at 393 nm as a function of time.^{20–23} Kinetic experiment was performed with **1** (at a constant concentration of 1×10^{-4} M) and 3,5-DTBC (varying the concentration from 1×10^{-3} M to 1×10^{-2} M) in acetonitrile using UV-Vis spectrophotometer. 2 mL of 3,5-DTBC solution at appropriate concentration, obtained by accurate dilution from the stock solution, was taken in the UV-Vis quartz cell (1 cm) and kept for a while inside the cell holder which was attached with a thermostat to keep the temperature at 25°C. Then, 0.04 mL of stock solution of the complex was added to it to achieve the ultimate concentration of the complex as 1×10^{-4} M. The formation of 3,5-DTBQ was monitored with time at a wavelength of 393 nm. Each experiment was performed in triplicate.

2.6 Detection of hydrogen peroxide in the catalytic oxidation of 3,5-DTBC

To detect the formation of hydrogen peroxide during the catalytic reaction, we followed a previously reported

method.²⁴ Reaction mixtures were prepared as in the kinetic experiments. During the course of the oxidation reaction, the solution was acidified with H_2SO_4 to pH 2 to stop further oxidation after a certain time and an equal volume of water was added. The formed quinone was extracted three times with dichloromethane. 1 mL of 10% solution of KI and three drops of 3% solution of ammonium molybdate were added to the aqueous layer. The formation of I^{3-} could be monitored spectrophotometrically because of the development of the characteristic I^{3-} band ($\lambda_{max} = 353$ nm, ϵ (extinction coefficient) = $4741 \text{ M}^{-1}\text{cm}^{-1}$).

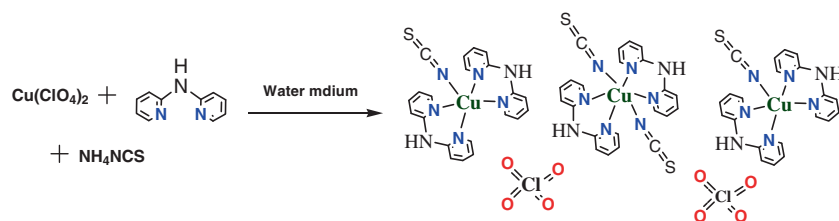
3. Results and Discussion

3.1 Synthesis and formulation

The hetero-geometric discrete copper(II) complex (**1**) was synthesized by addition of 2,2'-dipyridylamine to a solution of $Cu(ClO_4)_2 \cdot 6H_2O$ followed by the addition of ammonium thiocyanate (NH_4SCN) in aqueous solution at room temperature (Scheme 1). The structural formulation was determined by using routine spectroscopic techniques including single crystal X-ray diffraction analysis.

3.2 Description of crystal structure

The X-ray crystal structure analysis of **1** reveals that hetero-geometric copper(II) complex (**1**) crystallizes in monoclinic crystal system with $P2_1/c$ space group.



Scheme 1. Synthesis of the copper(II) complex.

An ORTEP of the copper complex is shown in the Figure 1. Two isostructural independent monocationic, $[\text{Cu}(\text{dpa})_2\text{NCS}]^+$ units and one *trans*- $[\text{Cu}(\text{dpa})_2(\text{NCS})_2]$ unit crystallized through $\text{S} \cdots \text{H}$ bonds and the residual two units of cationic charge, is counterbalanced by two perchlorate ions in the unit cell. Between the two hetero-geometric copper centers, Cu2 center is in octahedral geometry and the primary zone of Cu2 is coordinated by nitrogen atoms of the dipyridyl ligands in equatorial plane [Cu2-N8 = 2.020(3) Å, Cu2-N10 = 2.004(3) Å] with two axially occupied thiocyanate ligands, Cu2-N1 = 2.494(6) Å. In the complex unit, the geometry of cationic Cu1 unit may be best described as distorted square pyramidal (Figure 1) as evident from the value of the trigonal index, $\tau = 0.063$; [$\tau = |\beta - \alpha|/60$], where $\alpha = 90^\circ$ and $\beta = 93.802^\circ$; τ is 1 for a perfect trigonal bipyramidal geometry and is zero for a perfect square pyramidal geometry.²⁴ In the Cu1 complex unit, one of the two bidentate dipyridylamine ligands coordinates to Cu(II) center at apical [Cu1-N3 = 2.138(4) Å, and equatorial [Cu1-N1 = 2.020(4) Å] sites and the other dipyridylamine chelates to Cu(II) ions at equatorial positions [Cu1-N4 = 1.992(4) Å, Cu1-N6 = 2.012(4) Å]. The last equatorial site at Cu1 ions was coordinated by N-atom of the isothiocyanate groups [Cu1-N7 = 1.995(4) Å].

Molecular packing diagram of **1** indicates that square pyramidal copper (Cu1) units coexist with octahedral

copper (Cu2) units through weak forces in solid state (Figure S1). Close observation of **1** suggests that Cu2 center acts as a center of inversion in the unit cell. Cu1 unit is attached with Cu2 unit *via* moderately strong H-bonding between sulphur atoms of terminal thiocyanate ions and hydrogen atoms [H(2) \cdots S2, 2.73 Å; H(4) \cdots S2, 2.85 Å; Figure S2 (see Supplementary Information)].

3.3 Electronic and EPR spectral characterization

The integrity of the copper complex in solution was checked through UV-Vis and EPR spectral analysis. The UV-Vis spectrum for **1** in acetonitrile at room temperature shows a series of high intensity transitions in the range of 250 to 269 and 290 to 320 nm (Figure S3 in Supplementary Information) which are attributed from the intraligand transitions. A very broad low energy transition centered at 682 nm (Figure S3 in Supplementary Information) is assigned to the ligand field transition for the copper complex. The X-band EPR spectra of the copper complex (Figure S4 in Supplementary Information) at room temperature (RT) and low temperature (LT) were recorded in MeCN solution and examined to distinguish the hetero-geometry of copper centers in **1**. Complex **1** consists of a three copper centers, with two being in square pyramidal and one in octahedral environment. However, the room temperature spectrum

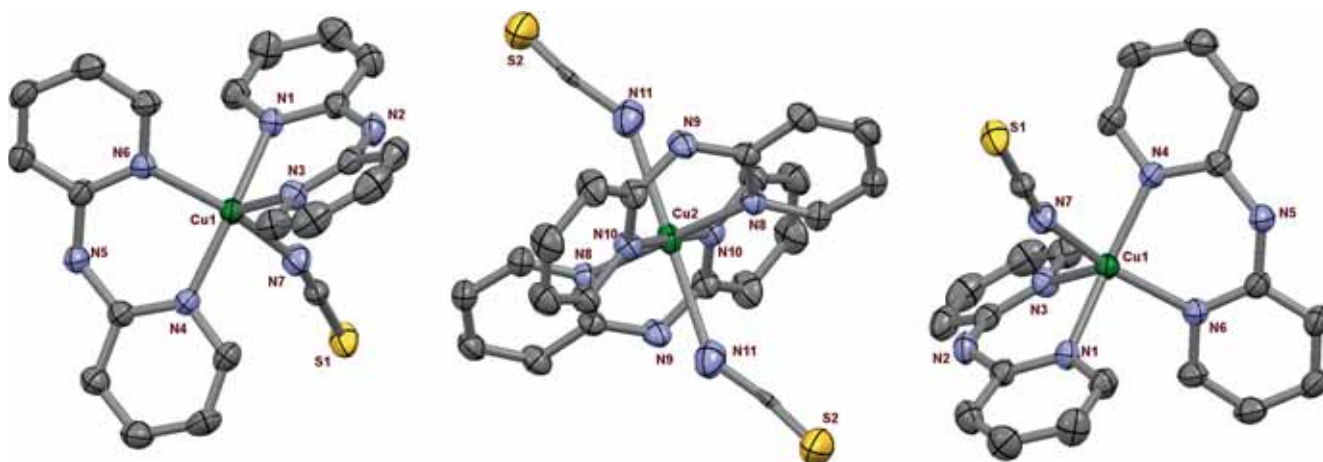


Figure 1. ORTEP of 1^{2+} with 30% ellipsoid probability.

showed the presence of a single species which was confirmed by simulating the spectrum (Figure S4 in Supplementary Information). This behavior could be understood since the three copper nuclei might behave as exchange couples so as to form a single species with a new spin state $S = 1/2$. Low temperature experiments were also performed but were not helpful in differentiating the coordination environments of the metal centers. LT spectral analysis reveals the presence of four lines in the spectrum.

3.4 Catechol oxidation activity

The catalytic activities of **1** towards a standard substrate 3,5-di-*tert*-butylcatechol (3,5-DTBC) in acetonitrile medium under aerobic condition have been studied. Spectrophotometric scans revealed a gradual decrease in intensity of the band at 284 nm due to the gradual decline of catechol^{25,26} and an appearance of a new band with increasing intensity at ~ 393 nm (Figure 2). The corresponding quinone (3,5-DTBQ) was purified by column chromatography and isolated in high yield (83.8% for **1**) by slow evaporation of the eluent. The

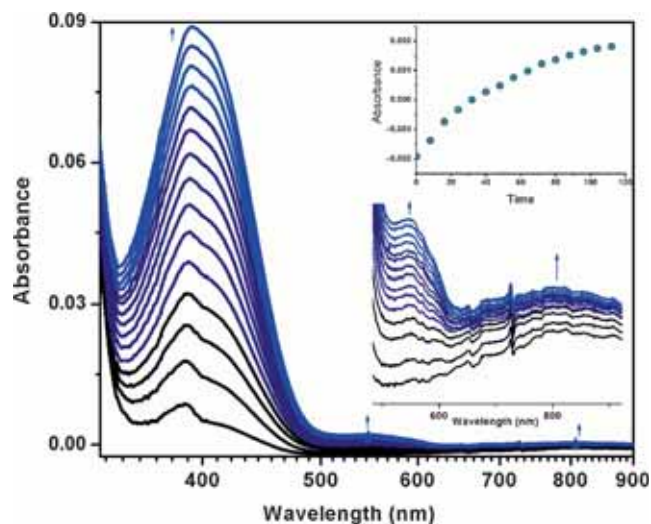


Figure 2. Increase of quinone band at 393 nm after addition of 100 equivalents of 3,5-DTBC to a solution containing **1** (10^{-4} M) in acetonitrile at 25°C path length, 1 cm. The spectra were recorded at an interval of 5 min. Inset (bottom): Expanded plot. Inset (Top): Absorbance at 807 nm vs time plot to reveal the nature of oxidation reaction.

product was identified by ^1H NMR spectroscopy. ^1H NMR (CDCl_3 , 400 MHz) δ_{H} : 1.19 (s, 9H), 1.22 (s, 9H), 6.14 (d, $J = 2.4$ Hz, 1H), 6.96 (d, $J = 2.4$ Hz, 1H). The kinetics of oxidation of 3,5-DTBC by **1** were determined by the method of initial rates which involved monitoring the growth of the quinone band at 393 nm as a function of time.^{22–24} The rate constant versus concentration of the substrate data were then analyzed on the basis of the Michaelis–Menten approach of enzyme kinetics to get the Lineweaver–Burk plot (double reciprocal), as well as the values of the parameters V_{max} , K_{M} , and k_{cat} . The observed rate constant versus substrate concentration plot for **1** in MeCN is shown in Figure S5 (see Supplementary Information). The kinetic parameters for **1** are listed in Table 3.

3.5 Mechanistic aspects of catecholase activity

Irreversible reduction and oxidation peaks for **1** were observed at -780 and $+35$ mV (Figure 3) at the scan rate of 20 mV s^{-1} suggesting that the reduction is quite difficult due to increase in the electron density significantly on central Cu(II) ion. To gain mechanistic insight of catechol oxidation by the Cu(II) complex, we have performed electrochemical analysis of the oxidation of 3,5-DTBC in presence and absence of the copper complex under aerobic atmosphere. A mixture containing one part of the complex and 100 parts of 3,5-DTBC were analysed by cyclic voltammetry without the purging of argon gas.²⁴ The cyclic voltammogram of 3,5-DTBC in presence of **1** (Figure 3) shows a reduction and an oxidation peak at -475 , and $+545$ mV with significant increase in the reduction peak current (Figure 3). An oxidation hump at approx. $+270$ mV for **1** in presence of 3,5-DTBC appeared due to the oxidation of Cu(I) which is generated in the catalytic pathway. The absence of the reduction peak of Cu(II) in the cyclic voltammogram of 3,5-DTBC in the presence of copper complex is indicative of the reduction of Cu(II) to Cu(I) during the course of electro-catalytic effect of the complex in which the 3,5-DTBC is oxidized to quinone.

The result of electrochemical analysis was further confirmed by EPR analysis. The room temperature X-band frequency EPR spectrum of the complex (Figure 4) consists of quartet hyperfine structure

Table 3. Kinetic parameters for the catechol oxidation by **1**.

Solvent	V_{max} (M s^{-1})	Std. error	K_{M} (M)	Std. error	k_{cat} (h^{-1})	References
MeCN	1.33×10^{-4}	2.82×10^{-5}	7.34×10^{-3}	4.8×10^{-3}	4.788×10^3	This paper
TRIS buffer	9.63×10^{-4}	–	1.33×10^{-4}	–	63	27
TRIS buffer	8.9×10^{-5}	–	1.33×10^{-4}	–	5.06×10^2	27

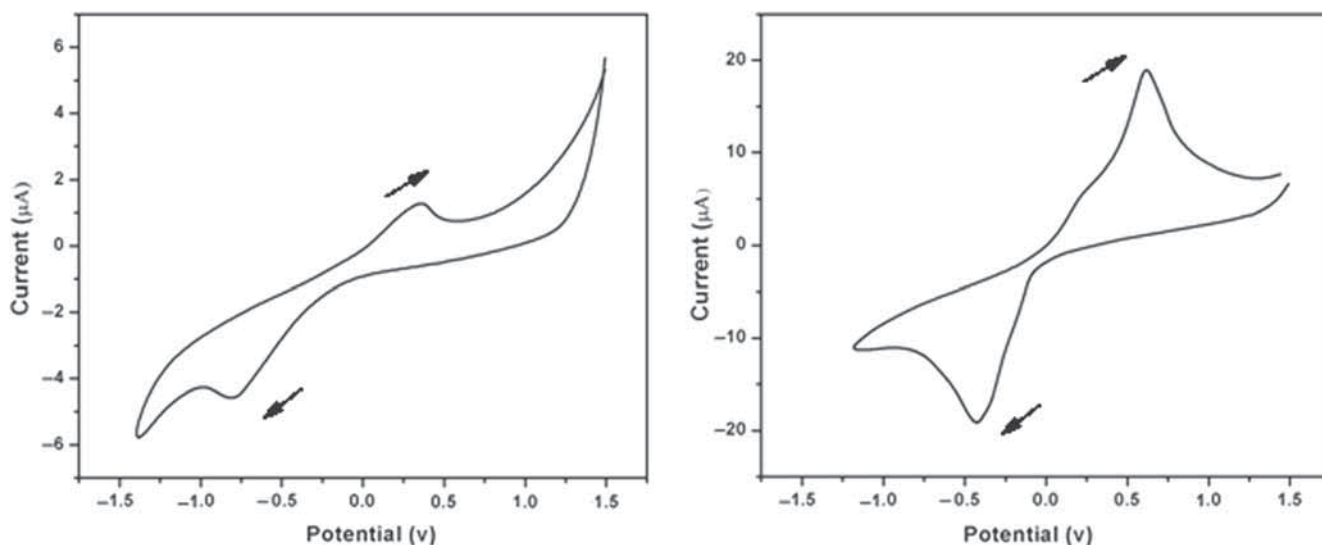


Figure 3. Cyclic voltammogram of Cu complex (Left) and (Right) Cu complex with 3,5-DTBC mixture in acetonitrile solution containing 0.1 M TBAP at 25°C using Ag/AgCl reference electrode. Scan rate: 20 mV s⁻¹. [Cu-complex] = 10⁻³ M, [3,5-DTBC] = 0.1 M, [NaF] = 0.1 M, T = 298.15 K.

exhibiting m_1 -dependent line widths, typically of copper (II) undergoing tumbling motion (**1**, $A_{\text{iso}} = 57$ G). In order to detect the presence of organic radical, if any, produced as intermediate species and to understand the redox participation of the metal centers, we have recorded the X-band EPR spectra of the copper complex in acetonitrile solution of 3,5-DTBC. The shape of the X-band EPR spectra of copper complex after addition of large excess of 3,5-DTBC (>1000 fold) to 10⁻⁴ M solution of **1** in acetonitrile recorded at room temperature were similar to complexes in acetonitrile that is without addition of 3,5-DTBC (no change in g and A value for Cu²⁺) except for a weak signal due to 3,5-DTBC radical developed at g ca 2.0049. However, the intensity of EPR spectral lines for Cu²⁺ decreases with time and simultaneously a new single line (red coloured) appears with time. The reported g value for oxidised DTB radical (semiquinone) is 2.0051 in 10⁻¹ M Bu₄NPF₆.²⁷ Thus, we assign the single line at 3450 G to the semiquinone radical. It is important to note that the shape of the signal decreases uniformly which is assignable to the *unselective* reduction of copper(II). The reaction was also followed in the presence of a radical scavenger, TEMPO (TEMPO = 2,2,6,6-tetramethylpiperidinoxyl). Notably, no oxidation of catechol was observed in the presence of two equivalent of TEMPO with respect to the copper complex used. This result further confirms that catechol oxidation is catalyzed by the cationic Cu(II) units and indicated by radical generation (Scheme 2).

In the two proposed mechanisms,^{3a,7,8} the monodentate asymmetric coordination of the substrate has been proposed in Krebs's mechanism,^{7,8} whereas

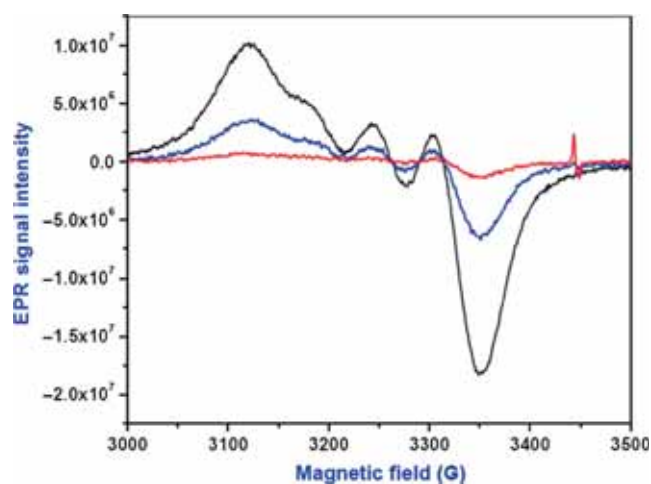
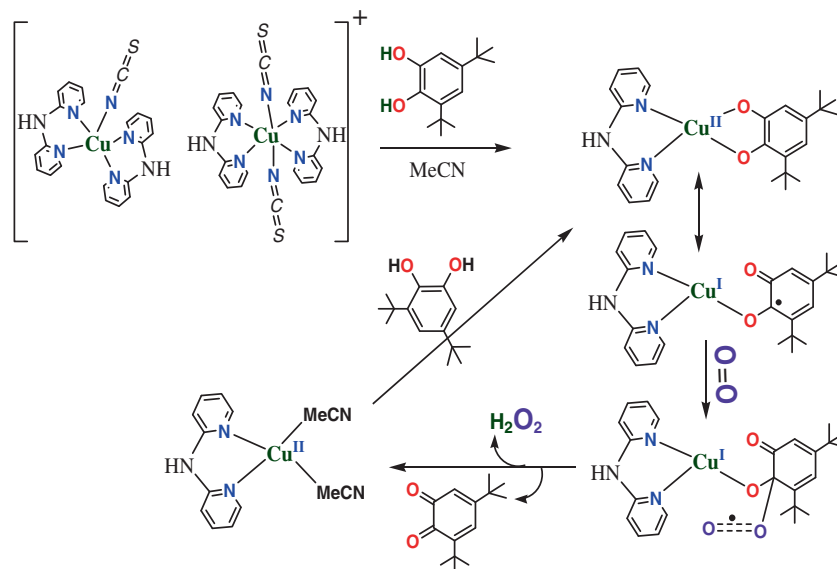


Figure 4. EPR spectra of Cu complex **1** (10⁻⁴ M) recorded at different time intervals after addition of 3,5-DTBC (excess) in acetonitrile. (a) black, $t = 0$ sec; (b) blue, $t = 2$ min; (c) red, 20 min. All EPR spectra were recorded at room temperature. The single line appearing in EPR spectrum (red) at 3450 G corresponds to the semiquinone radical.

simultaneous coordination of the substrate to both the copper centers (dinucleating bridging fashion) is suggested in the Solomon's mechanism.^{3a} The ESI mass spectrum of the reaction mixture of a 1:100 ratio of copper complex and 3,5-DTBC in acetonitrile (Figure S6) exhibits the base peak at $m/z = 243.10$ for **1** corresponding to the quinone sodium aggregate, [3,5-DTBQ-Na]⁺. The peaks at $m/z = 455.14$ and 486.9 corroborate the formation of [Cu(dpa)(DTBC)-H]⁺ and [Cu(dpa)(DTBC)(O₂)-H]⁺ species respectively, as intermediates. To investigate the efficiency of the catalytic activity we draw a comparison between our Cu(II) complex



Scheme 2. Mechanistic aspects of catechol oxidation by Cu complex.

and a dinuclear copper complex with distant metal centers.²⁸ This comparison indicates that the hetero-geometric copper(II) complex acts as a better and more effective catalyst towards catecholase activity than the reported one.²⁸ Presence of multiple metal centers towards catecholase activity enhances the rate of catalytic oxidation in a significant manner since the availability of metal centers increases the possibility of formation of enzyme-substrate adduct which is fundamental for the catalytic oxidation by metal complexes.

4. Conclusions

In summary, though, similar types of structure are previously reported but herein, we report the novel addition of a new class of catalytic systems as discrete hetero-geometric Cu(II) complexes containing dipyriddyamine ligands and thiocyanate, $[\text{Cu}(\text{dpa})_2\text{NCS}]_2[\text{Cu}(\text{dpa})_2(\text{NCS})_2](\text{ClO}_4)_2$ (**1**) which potentially mimics the full catalytic cycle of functional models of the active site of catechol oxidase enzyme with turnover number, $4.788 \times 10^3 \text{ h}^{-1}$ along with the production of benzoquinone and hydrogen peroxide. The generation of Cu(I) species in the catalytic pathways established by electrochemical analysis is further confirmed by electron paramagnetic resonance (EPR) spectroscopy. EPR analysis of the catechol in presence of Cu complexes indicates the generation of DTBC radical in solution and this radical plays the key role for promoting the aerobic oxidation of 3,5-DTBC to 3,5-DTBCQ. Existence of isolated Cu^{II} complex units in the course of catalysis significantly accounts for the reactivity of this complex.

Supplementary information (SI)

CCDC 1456703 contains the supplementary crystallographic data for **1**. These data can be obtained free of charge via <http://www.ccdc.cam.ac.uk/conts/retrieving.html>, or from the Cambridge Crystallographic Data Centre, 12 Union Road, Cambridge CB2 1EZ, UK; fax: (+44) 1223-336-033; E. mail: deposit@ccdc.cam.ac.uk

All additional information pertaining to molecular packing diagram, H-bonding interaction, UV-Vis spectrum, EPR spectra at RT and LT, plot of substrate concentration vs. rate, and ESI mass spectrum of the reaction mixture are given in the supporting information available at www.ias.ac.in/chemsci.

Acknowledgements

The work is supported financially by the Science and Engineering Research Board (SERB), New Delhi, India under FAST TRACK SCHEME for YOUNG SCIENTIST (NO. SB/FT/CS-088/2013 dt. 21/05/2014). ARC thanks IISER Mohali for the X-ray facility available at the Department of Chemical Sciences. HRY thanks UGC, India for fellowship.

References

1. W Kaim and B Schwederski 1991 (Eds.) *Bioanorganische Chemie* (Stuttgart: Teubner)
2. Que L Jr 1993 In *Bioinorganic Catalysis* J Reedijk (Ed.) pp. 347–393 (New York: Marcel Dekker)
3. Simándi L I 1992 *Advances in Catalytic Activation of Dioxygen by Metal Complexes* (Dordrecht, Boston, London: Academic Publishers)

4. (a) Solomon E I, Sundaram U M and Machonkin T E 1996 *Chem. Rev.* **96** 2563; (b) G Parshall and S Iittel 1992 (Eds.) *Homogeneous Catalysis* 2nd edition (New York: John Wiley); (c) Biswas B, Al-Hunaiti A, Räisänen MT, Ansalone S, Leskelä M, Repo T, Chen Y-T, Tsai H-L, Naik A D, Railliet A P, Garcia Y, Ghosh R and Kole N 2012 *Eur. J. Inorg. Chem.* 4479
5. Decker H, Dillinger R and Tuzcek F 2000 *Angew Chem.* **112** 1656
6. Schindler S 2010 *Eur. J. Inorg. Chem.* 2311
7. Eicken C, Zippel F, Buldt-Karentzouloulos K and Krebs B 1998 *FEBS Lett.* **436** 293
8. Eicken C, Krebs B and Sacchettini J C 1999 *Curr. Opin. Struct. Biol.* **9** 677
9. Klabunde T, Eicken C, Sacchettini J C and Krebs B 1998 *Nature Struct. Biol.* **5** 1084
10. Ackermann J, Meyer F, Kaifer E and Pritzkow H 2002 *Chem. Eur. J.* **8** 247
11. Kupán A, Kaizer J, Speier G, Giorgi M, Réglie M and Pollreis F 2009 *J. Inorg. Biochem.* **103** 389
12. Majumder S, Sarkar S, Sasmal S, Sañudo E C and Mohanta S 2011 *Inorg. Chem.* **50** 7540
13. Youngme S, Phuengphai P, Chaichit N, Mutikainen I, Turpeinen U and Murphy B M 2007 *J. Coord. Chem.* **60** 131
14. Mesa J L, Urtiaga K, Lezama L and Arriortua M I 1999 *Acta Chem. Scand.* **53** 634
15. Sletten J, Svardal K and Sørensen A 1993 *Acta Chem. Scand.* **47** 1091
16. *CrystalClear 2.0*; Rigaku Corporation: Tokyo, Japan
17. Sheldrick G M 2008 *Acta Cryst.* **A64** 112
18. Dolomanov O V, Bourhis L J, Gildea R J, Howard J A K and Puschmann H 2009 *J. Appl. Cryst.* **42** 339
19. Nardelli M 1983 *Comp. Chem.* **7** 95
20. Dey D, Kaur G, Ranjani A, Gyathri L, Chakraborty P, Adhikary J, Pasan J, Dhanasekaran D, Choudhury A R, Akbarsha M A, Kole N and Biswas B 2014 *Eur. J. Inorg. Chem.* 3350
21. Pal S, Chowdhury B, Patra M, Maji M and Biswas B 2015 *Spectrochim. Acta Part A* **144** 148
22. Basu P K, Mitra M, Ghosh A, Thander L, Lin C-H and Ghosh R 2014 *J. Chem. Sci.* **126** 1635
23. (a) Dey D, De A, Pal S, Mitra P, Ranjani A, Gayathri L, Chandraleka S, Dhanasekaran D, Akbarsha M A, Kole N and Biswas B 2015 *Ind. J. Chem. A* **54** 170; (b) Kannappan R, Mahalakshmy R, Rajendiran T M, Venkatesan R and Rao P S 2003 *J. Chem. Sci.* **115** 1
24. Dey D, Das S, Yadav H R, Ranjani A, Gyathri L, Roy S, Guin P S, Dhanasekaran D, Choudhury A R, Akbarsh M A and Biswas B 2016 *Polyhedron* **106** 106
25. Tsuruya S, Yanai S-I and Masai M 1986 *Inorg. Chem.* **25** 141
26. Zippel F, Ahlers F, Werner R, Haase W, Nolting H-F and Krebs B 1996 *Inorg. Chem.* **35** 3409
27. Hartl F 1995 *Inorg. Chim. Acta* **232** 99
28. Mendoza-Quijano M R, Ferrer-Sueta G, Flores-Álamo M, Aliaga-Alcalde N, Gómez-Vidales V, Ugalde-Saldívar V M and Gasque L 2012 *Dalton Trans.* **41** 4985